JOURNAL OF APPLIED ELECTROCHEMISTRY 22 (1992) 927–934

Aqueous polysulphide flow-through electrodes: effects of electrocatalyst and electrolyte composition on performance

P. M. LESSNER*, F. R. McLARNON, J. WINNICK‡, E. J. CAIRNS

Applied Science Division, Lawrence Berkeley Laboratory and Department of Chemical Engineering, University of California, Berkeley, CA 94720, U.S.A.

Received 6 December 1991; revised 17 February 1992; accepted 18 February 1992

Porous electrodes are required to achieve satisfactory performance of the aqueous sulphide/polysulphide redox couple in energy conversion and storage applications. A flow cell for testing flow-through porous electrodes was constructed and operated. The effects of electrode material, temperature, flow rate, and electrolyte composition were studied. Catalytic electrode surface layers of Co and MoS_2 demonstrated performances which were more than adequate to meet a design goal of 10–20 mA cm^{-2} at less than 50 mV overpotential. Flow rate variation had only a small effect on the current density–overpotential behaviour, whereas raising the temperature and/or adding dimethylformamide to the electrolyte had much larger effects. These observations are consistent with steady-state results obtained on rotating disc electrodes.

Nomenclature

a_0	Interfacial area per unit volume (cm^{-1})
A	area (cm^2)
d	wire diameter (cm)
D	diffusion coefficient ($cm^2 s^{-1}$)
F	Faraday (96 487 C mol^{-1})
i	current density (A cm^{-2})
L	defined by Equation 5 (cm)
m	mesh size (wires/cm)
m_0	mass transfer coefficient (cm s^{-1})
n	number of electrons
Q	volumetric flow rate (cm^3 sec^{-1})
Re	Reynolds number
w	mass (g)

Greek symbols

δ	electrode thickness (cm)
ε	porosity or open area ratio
μ	viscosity (g cm^{-1} s^{-1})
ρ	density (g cm^{-3})

Subscripts

b	bulk
e	electrolyte
i	species i
L	limiting

Abbreviations

DMF	dimethylformamide
FEP	fluorinated ethylenepropylene
PEC	photoelectrochemical cell
PTFE	polytetrafluoroethylene

1. Introduction

The aqueous polysulphide redox couple has shown promise for use in both energy conversion (photoelectrochemical cells (PECs)) and energy storage (redox batteries). Both applications require the redox electrode to exhibit small overpotentials at large current densities in order to achieve efficient cell operation. A reasonable design goal for energy storage and conversion applications is for the electrode to operate at 10–20 mA cm^{-2} at an overpotential of less than 50 mV.

Recent chemical [1, 2] and spectroscopic [3–6] investigations have shown that S_4^{2-} is the major polysulphide species over the range of compositions of interest in photoelectrochemical work. The major monosulphide species is HS^- (bisulphide). Thermodynamic data [7, 8] suggest that polysulphide redox reactions in alkaline electrolytes can be represented by the reaction

$$S_4^{2-} + 4H_2O + 6e^- \rightleftharpoons 4HS^- + 4OH^- \quad (1)$$

We reported on the kinetics of the polysulphide redox couple at a dark electrode in a previous series of papers [9–11]. It was demonstrated [10] that Reaction 1 can be split into a homogeneous solution-phase reaction that produces the supersulphide ion S_2^-:

$$S_4^{2-} \rightleftharpoons 2S_2^- \quad (2)$$

and a heterogeneous electrochemical reaction:

$$2S_2^- + 4H_2O + 6e^- \rightleftharpoons 4HS^- + 4OH^- \quad (3)$$

* Present address: W. R. Grace/Chromerics, Inc., 77 Dragon Court, Woburn, MA 01888, U.S.A.
‡ Present address: Georgia Institute of Technology, School of Chemical Engineering, Atlanta, GA 30332, U.S.A.

0021-891X/92 © 1992 Chapman & Hall

Reaction 3 is a multistep reaction comprising elementary chemical and electrochemical steps. The kinetics at a photoanode have been found [12] to conform to the same reaction scheme as at the dark cathod.

Aqueous polysulphide solutions used in photoelectrochemical cells must have both sulphur (present as polysulphide) and sulphide (present as bisulphide or polysulphide) in quantities that will support current densities in excess of $10\,mA\,cm^{-2}$. It has been found empirically that concentrations in the order of 1 M are needed for both sulphur and sulphide. An optimum solution composition would have a high electrochemical kinetic activity and would only undergo disproportionation to thiosulphate slowly.

Our previous kinetic and mass transfer studies [10, 11] showed that the current density at an electrode carrying out the sulphide/polysulphide redox reaction is limited by the combined effects of reactions in solution and slow electrochemical kinetics (at low cathodic overpotentials). It was shown that the addition of 13 mol % dimethylformamide (DMF) to the aqueous polysulphide solution significantly increased the current density, at a given temperature and overpotential, by increasing the equilibrium concentration of S_2^- (driving Reaction 2 to the right). An examination of the rotating disc data presented in [11] shows that a design goal of supporting $10–20\,mA\,cm^{-2}$ with an overpotential of less than 50 mV at the counter-electrode of a PEC cannot be met at a smooth planar electrode. For example, at 77°C, the current density at $-50\,mV$ polarization on a smooth cobalt electrode is $-2.5\,mA\,cm^{-2}$ in aqueous solution and $-6.4\,mA\,cm^{-2}$ in a solution with 13 mol % DMF added. An increase in current density of 3 to 5 times is needed in order to meet the design goals.

Porous electrodes consist of a solid phase and a liquid phase in intimate contact, and therefore have a high interfacial area per unit volume (a_0). Porous electrodes have been used for removal of materials from waste streams [13], in redox batteries [14], and in stationary battery electrodes [15]. The electrode structure can be invariant with time as in most redox battery and fuel cell applications, or solid reactants can be part of the electrode matrix (for example in most secondary batteries). Mass transfer in the liquid phase can take place by diffusion, migration, natural convection and/or forced convection.

In our case, an electrode that carries an electric current and acts as an electrocatalyst, yet does not change its structure with time, is desired. A metal or metal sulphide deposited on a wire screen or expanded-metal mesh should meet these requirements, and a structure of this type could be used as a flow-through electrode. Electrolyte flow would be useful in a redox battery employing the aqueous polysulphide electrolyte, because in redox batteries the electrolyte is typically stored in a location remote from the cell stack, or in a PEC, where flow could be used to facilitate the removal of waste heat.

This paper describes the preparation and testing of electrocatalytic porous electrodes for the aqueous polysulphide redox system, and the construction and operation of a flow cell. The effects of different catalyst materials, temperature, and addition of DMF are investigated. These results are compared with previous kinetic and mass transfer studies at planar electrodes in similar electrolytes.

2. Experimental details

2.1. *Cell and flow system construction*

A cross-sectional view of the cell is shown in Fig. 1. Fluoropolymers such as PTFE, FEP and PFA were used as materials of construction wherever practical, and the cell body was fabricated from PTFE. The flow channel was 2.54 cm in diameter (cross-sectional area $5.07\,cm^2$), and the electrolyte entered through the bottom of the cell. To ensure uniform flow distribution, and prevent channeling, a flow distributor of quartz (sand) particles was placed 0.5 cm above the inlet. The sand was composed of irregularly shaped particles 0.5 to 1 mm in diameter, resulting in a column-to-particle diameter ratio of greater than 25, and the packed depth of the sand was 0.75 cm. Pt–10% Rh screens (80-mesh) held the sand in place, and the screens were sandwiched between PTFE washers for mechanical stability.

A type K thermocouple (Ni–Cr/Ni–Al, Omega Engineering) was used to measure the temperature of the entering fluid. It was coated with 0.05 cm thick FEP in order to protect it from the corrosive electrolyte, and the thermocouple tip protruded about 3 mm into the fluid flow path. The reference electrode was a 3.18 mm diameter platinum rod (99.95%), which was sealed into a pipe plug that was mounted in a branch of a PTFE pipe tee. Part of the fluid entering the cell was tapped off to flow through the tee and over the reference electrode. This arrangement ensured that the reference electrode was at the same temperature as the working electrode.

The working electrode was held in place between a 4.76 mm lip in the body of the cell and a 1.25 cm long piston sleeve. A stack of screen electrodes up to 0.5 cm in height could be accommodated in the space between the lip and the piston sleeve. Electrical contact to the external circuit was made by a 0.50 mm (0.020 inch) diameter soft-temper platinum wire which was compressed between the piston sleeve and the electrode stack. The contact resistance between the wire and the working electrode was found to be negligible, so long as the working electrode was a metal.

The counter electrode had an external electrical contact which was similar to that used for the working electrode. A 1.25 cm long piston sleeve was placed on top of the electrode to hold it in place. An O-ring was pressed against the top of this piston sleeve and against the cell body by a 5 cm long piston sleeve with a conical taper cut into the end contacting the O-ring. This conical O-ring seal was found to be necessary to prevent electrolyte from leaking between the piston

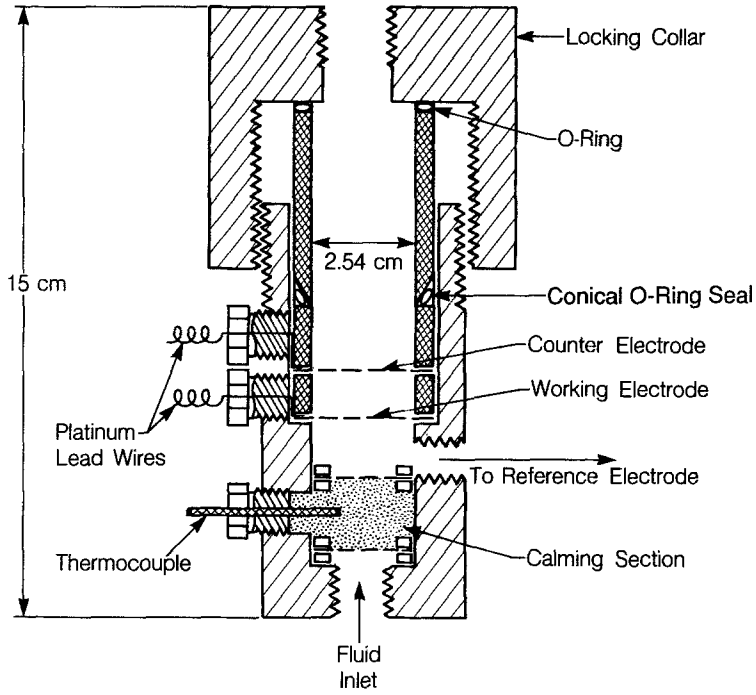

Fig. 1. Cross-section of the flow cell. The thermocouple and platinum lead wires are sealed into PTFE pipe plugs, which are mounted on the cell via 1/8 inch FNPT pipe threads tapped into the cell body.

sleeves and the cell body. A locking collar held the piston sleeves in place and provided compression for the O-ring seals and between the electrodes and contact wires.

A schematic diagram of the complete flow system is shown in Fig. 2. A 1 dm^3 PTFE tank acted as a storage reservoir for the electrolyte, and its volume was about twenty times that of the cell. The tank cover had an O-ring which was compressed against the top lip of the tank with an external flange. The suction line of the pump was connected to the bottom of the tank via a fitting, and another fitting connected to a common discharge line for the cell, bypass loop, and reference-electrode compartment. A third fitting was connected to a stopcock which could be used to either vent the system or allow the introduction of an inert gas above the liquid.

A positive-displacement pump (Fluorocarbon, Model Saturn SP-3000, PTFE wetted parts) was used to move the fluid through the system. Two PTFE needle valves were used to control the flow rate through the cell and bypass loop. The flow rate through the cell was measured by a glass rotameter (Omega Engineering, FL-215). The minimum flow rate that could be read precisely was about 0.1 $dm^3 min^{-1}$, and the maximum flow rate attainable (about 1.6 $dm^3 min^{-1}$) depended on the number of electrode screens, the electrolyte, and the temperature.

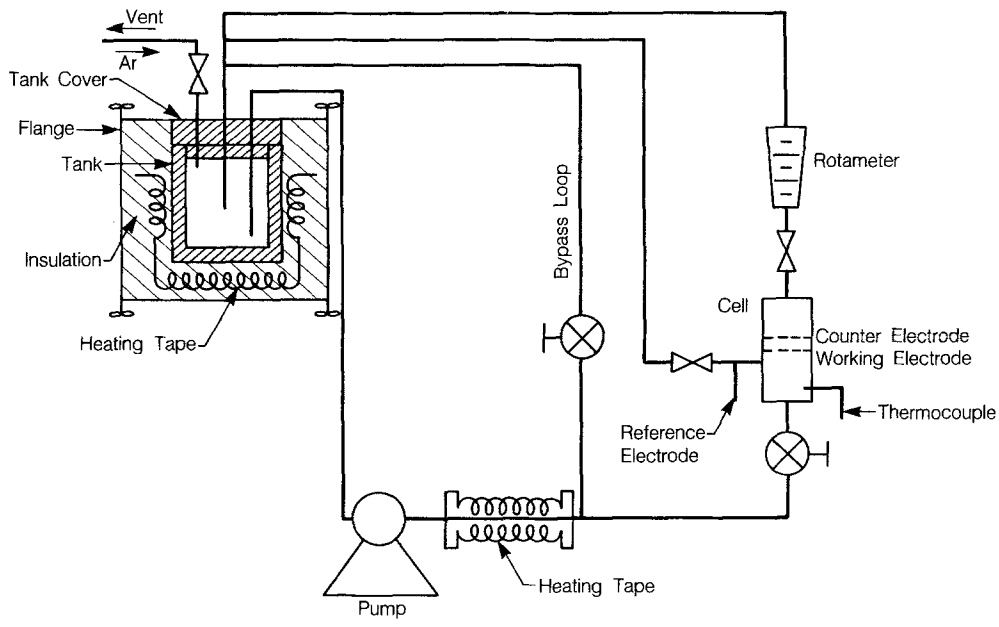

Fig. 2. Diagram of the flow system.

Table 1. Properties of screens and expanded metal

Material	*d* /mm	*δ* /mm	a_0 /cm^{-1}	*ε*	*Real Area / Projected Area*
Pt–10% Rh 80 × 80 mesh	0.076	0.200	75.7	0.82	1.51
Ni 100 × 100 mesh	0.114	0.254	122	0.67	3.10
Mo, 5-Mo 20–2/OE	0.127	0.381	–	0.78	–

Table 2. Cobalt plating bath and conditions

Plating bath composition		*Operating conditions*	
Component	*Concentration*	*Parameter*	*Value*
$CoCl_2 \cdot 6H_2O$	435 g dm^{-3}	Temperature	25 to 50° C
H_3BO_3	45 g dm^{-3}	Current density	40 mA cm^{-2}
		Plating time	140 min
		Cathodic period	40 ms
		Anodic period	8 ms

A stopcock was fitted between the top of the cell and the rotameter inlet, and during operation this stopcock was normally open. When changing electrodes this stopcock and the flow-control valves could be closed to allow the cell to be isolated from the rest of the system. Heating tape and thermal insulation were mounted on the outside of the pump discharge line, in order to minimize heat loss.

2.2. *Selection and preparation of electrocatalysts*

The electrocatalyst should be selected to be chemically and electrochemically stable, exhibit good electrocatalytic activity, and have a large active area per unit projected area. Prior work [16–19] showed that Co and MoS_2 should be considered for use as electrocatalysts. Nickel (or NiS_x) would be acceptable if its corrosion rate is small enough. Wire screen and expanded-metal mesh electrodes can provide the increase in surface area required to meet the design goals. For a square-weave wire mesh, the interfacial area per unit volume is given by [20]:

$$a_0 = \frac{2\pi m^2 dL}{\delta} \tag{4}$$

where

$$L = \left(\frac{d^2}{4} + \frac{1}{m^2}\right)^{1/2} \tag{5}$$

The open area ratio ε can be determined by weighing a sample of screen and using

$$\varepsilon = 1 - \frac{w}{\rho A \delta} \tag{6}$$

The real-to-projected area ratio of a single screen is given by:

$$\frac{\text{Real Area}}{\text{Projected Area}} = a_0 \delta \tag{7}$$

It can be seen that a single screen or a stack of a few screens should be able to meet the design requirements. Table 1 lists the properties of the screens and expanded-metal used in the present work.

The electrodes were punched from stock material by use of a 31.7 mm (1.25 inch) die punch. Cobalt screens were not available commercially, so cobalt was electroplated onto nickel screens. The plating bath composition is given in Table 2 [21], along with conditions for periodic-reversal plating. The nickel screens were degreased with soapy water, soaked in acetone, and then rinsed with distilled water before being electroplated with cobalt. The cobalt plate was approximately 25 μm thick, and it was bright and adherent. An SEM examination (Fig. 3) shows that the deposit was somewhat granular and rough.

For MoS_2, a semiconductor, to be an effective electrocatalyst it must be deposited on a conductive support. Layers of MoS_2 can be grown on molybdenum in a H_2S/H_2 [18] or sulphur [22] atmosphere. A molybdenum expanded-metal mesh (Exmet Corporation) and an excess of sulphur were placed in a quartz ampoule. The ampoule was sealed under a vacuum, and the contents were heated for 24 h at 450° C in a muffle furnace and then cooled slowly to room temperature. Calculations using the data in [22] predict that a layer about 0.7 μm thick will grow under these conditions. An adherent layer of MoS_2 was formed.

2.3 *Preparation of electrolyte*

The procedure for electrolyte preparation presented in [11] was modified in order to produce the greater quantities required (about 1.5 dm^3 for each run) for the flow cell experiments. A stock solution of twice the concentration of the working electrolyte was prepared. Water was deaerated by bubbling argon, and a vacuum was applied with an aspirator in order to remove as much of the dissolved argon as possible. After dissolving the calculated quantities of $Na_2S \cdot 9H_2O$ and sulphur in 750 cm^3 of water, the solution was placed in the PTFE tank. First air was swept out with argon, and then H_2S was used to

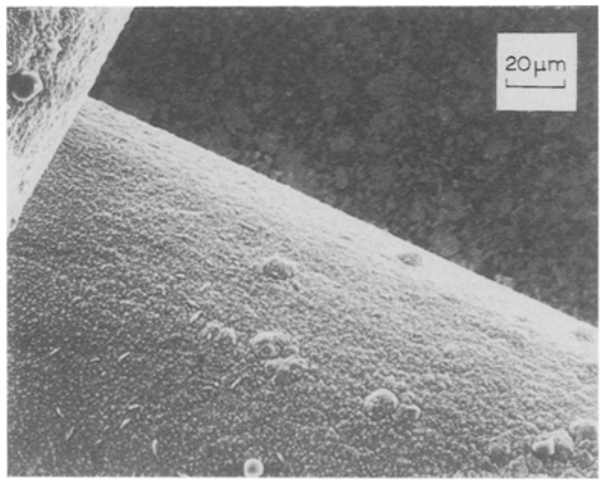

Fig. 3. Cobalt electrodeposit on a 40-mesh nickel screen.

displace the argon. The tank was pressurized with the H_2S to 6 p.s.i. (~ 40 kPa), and the solution in the tank was agitated with a magnetic stirrer while H_2S was absorbed from the vapour space above the solution. Samples were withdrawn at periodic intervals, and when the desired concentration was reached the flow of H_2S was stopped.

One-half of the stock solution was diluted with water, and the other half was diluted with a water-DMF mixture to bring the concentration of DMF to 13 mol %. Both working solutions were found to contain the same amount of total sulphur using the procedure outlined in [10]. The solutions were stored in 2 dm^3 polyethylene bottles under an argon atmosphere.

2.4. *Operating procedure*

To begin the experiment, the cell was assembled and connected to the flow system, and the tank was filled with electrolyte. During normal operation, argon gas was supplied to the vent valve. A pressure of 1–3 p.s.i. (~ 7–20 kPa) above the liquid in the tank was found to be helpful in preventing bubble formation at the pump inlet. Steady flow could be maintained for an indefinite period after adjustment of the two needle valves, and the temperature could be controlled to within ± 1° C for several hours.

Before changing electrodes the system was cooled to room temperature. All valves, including the normally-open stopcock at the cell outlet, were closed, and electrolyte was drained through the reference electrode line. The cell could then be disassembled, and the electrodes changed, while the rest of the system was protected from exposure to air.

3. Results and discussion

The electrochemical performance of the flow system was checked with 10 mM $K_3Fe(CN)_6/K_4Fe(CN)_6$ in 1 M KCl. Figure 4 shows the current density against overpotential (measured against the platinum reference electrode described above), at various flow rates, on a 80-mesh Pt–10% Rh screen. The potential was swept in the positive direction at 5 mV s^{-1}. In experiments that included a return sweep, no hysteresis was found.

The mass transfer coefficient can be calculated from the limiting current density plateau at each flow rate using

$$m_0 = \frac{i_L}{nFC_{ib}} \tag{8}$$

An appropriate definition for the Reynolds number for this geometry [23] is given by:

$$Re = \frac{\rho Q_e d}{\mu \varepsilon A} \tag{9}$$

where the characteristic dimension is the screen wire diameter. The dimensionless mass transfer rate (Sherwood number) is defined as:

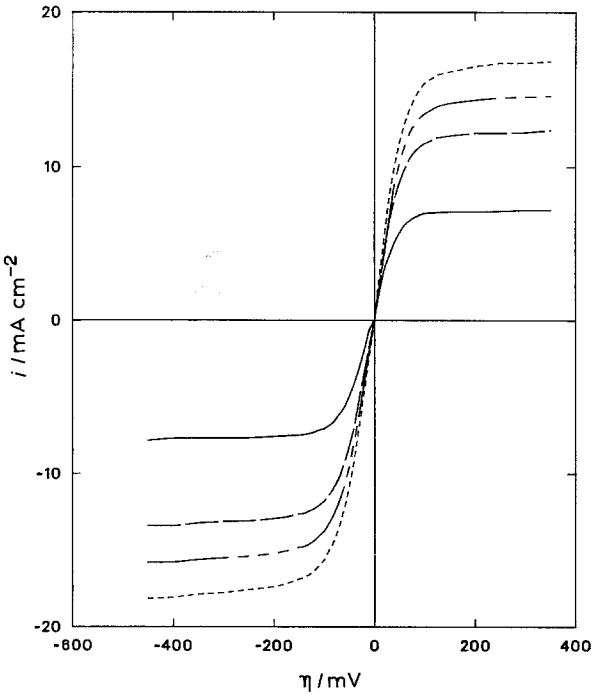

Fig. 4. Current density against overpotential on a 80-mesh Pt–10% Rh screen electrode in 10 mM $K_3Fe(CN)_6/K_4Fe(CN)_6$–1 M KCl electrolyte at 25° C and various flow rates: (——) 0.086; (– – –) 0.377; (——– – –) 0.685; and (- - - -) 1.002 $dm^3 min^{-1}$.

$$Sh = \frac{m_0 d}{D_i} \tag{10}$$

Based on the cathodic portion of the data presented in Fig. 4, the relationship between *Sh* and *Re* is given by:

$$Sh = 14.29\, Re^{0.348} \tag{11}$$

The functional dependence on *Re* is in excellent agreement with previous work [23, 24], however the constant term is slightly higher than values presented in these references. This deviation could be due to pump vibration or differences in physical properties between the liquids used here and the liquids used to derive the correlations.

Figures 5–7 show current density-overpotential curves obtained on molybdenum expanded-metal mesh on which MoS_2 has been deposited. Two expanded-metal screens were used as the working electrode. Due to the MoS_2 coating, a contact resistance of a few ohms was measured between the two electrodes. The electrolyte was 1.3 M S^{2-}, 1 M S^0 at pH 12. Figure 5 shows the response at 25° C and 46° C with and without the addition of 13 mol % DMF as a cosolvent, and Fig. 6 presents the corresponding results at 64° C and 80° C. As in the rotating disc experiments on cobalt and platinum [11], the addition of DMF increases the current density at a given overpotential and temperature. At low overpotentials, the current density using the solution with DMF at 23° C is approximately the same as the current density at 46° C using the solution with no DMF added. At all overpotentials, the current density at 64° C using the solution with DMF is greater than the current density at 80° C using the solution with no DMF. This result

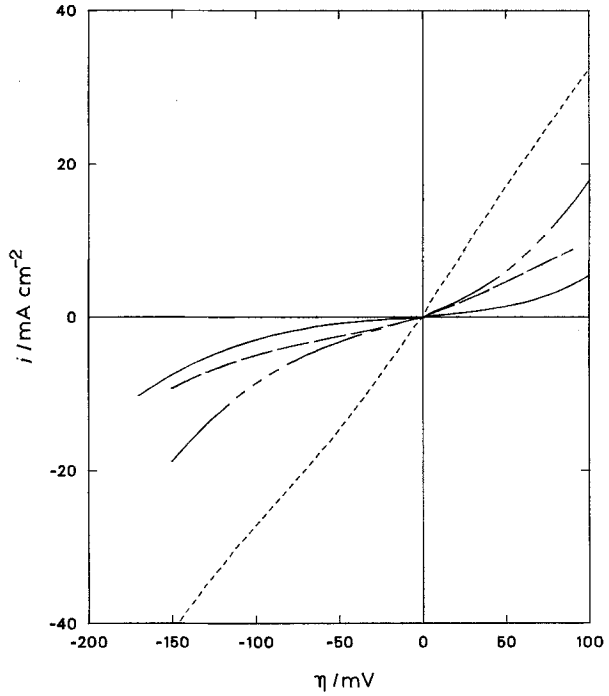

Fig. 5. Current density against overpotential on two Mo/MoS_2 expanded-metal screens at 23–47° C, with and without the addition of 13 mol % DMF. (——) 25° C, aqueous electrolyte; (– – –) 23° C, 13 mol % DMF added; (— — — —) 47° C, aqueous electrolyte; and (- - - -) 46° C, 13 mol % DMF added.

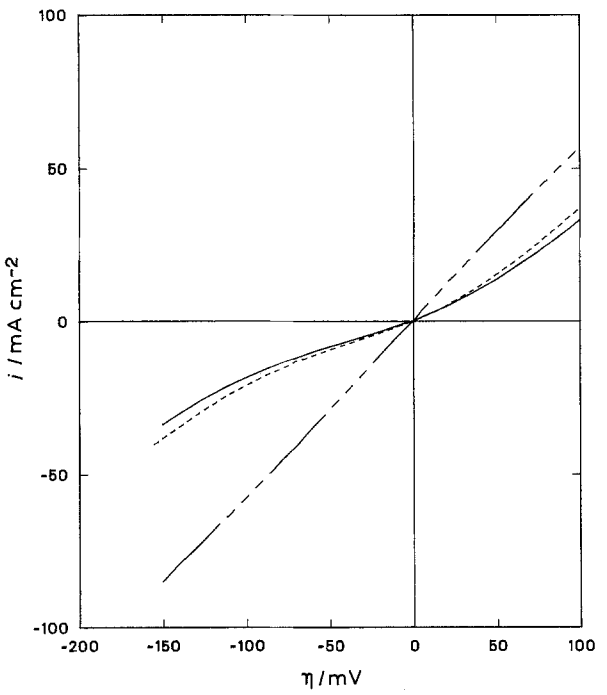

Fig. 7. Current density against overpotential on two Mo/MoS_2 expanded-metal screen electrodes at 64° C. Comparison of the effect of an increase in flow rate with an addition of 13 mol % DMF. (——) 0.1 $dm^3 min^{-1}$, 64° C, aqueous electrolyte; (– – –) 1 $dm^3 min^{-1}$, 64° C, aqueous electrolyte; and (— — — —) 1 $dm^3 min^{-1}$, 64° C, 13 mol % DMF added.

is consistent with our prior kinetic and mass transfer studies [9–11], which showed that the addition of DMF to the electrolyte increases the overall reaction rate by driving Reaction 2 to the right.

Figure 7 compares the effect of flow rate and DMF addition at 64° C. Changing the flow rate by an order of magnitude 0.1–1.0 $dm^3 min^{-1}$ gave a small increase in current density. The addition of DMF resulted in a much larger increase in current density than that produced by an order-of-magnitude increase in the flow rate.

Five 100-mesh nickel screens were tested in aqueous polysulphide solution containing 1.3 M S^{2-} and 1 M S^0 at a pH of about 13.8. Figure 8 shows how the res-

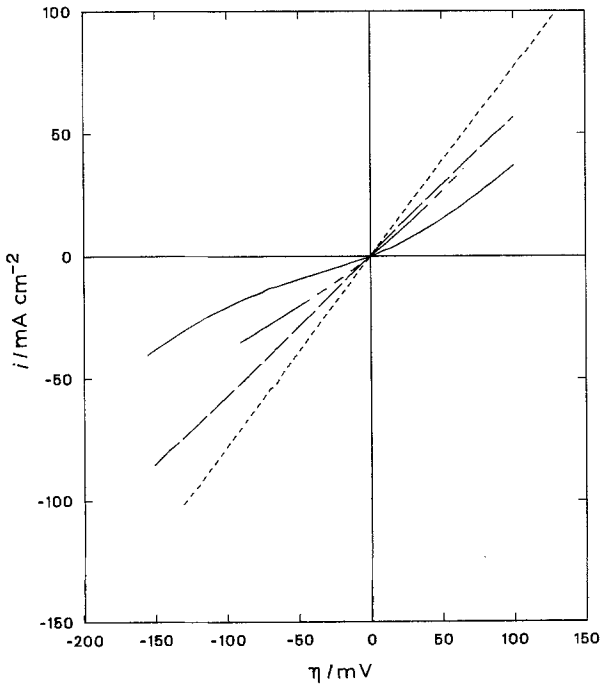

Fig. 6. Current density against overpotential on two Mo/MoS_2 expanded-metal screen electrodes at 64–80° C, with and without the addition of 13 mol % DMF. (——) 64° C, aqueous electrolyte; (– – –) 64° C, 13 mol % DMF added; (— — — —) 80° C, aqueous electrolyte; and (- - - -) 78° C, 13 mol % DMF added.

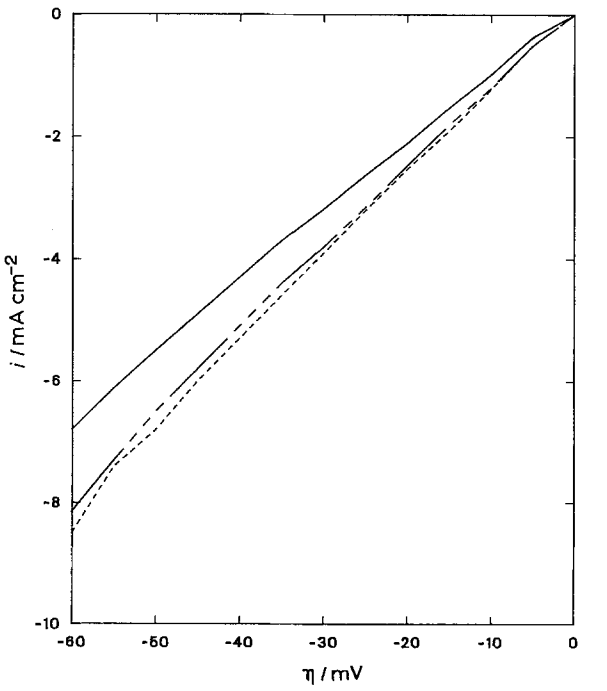

Fig. 8. Current density against overpotential on five 100-mesh nickel screen electrodes. Comparison of the effect of repeated potential scans. (——) initial response; (— — — —) third scan; and (– – –) sixth scan.

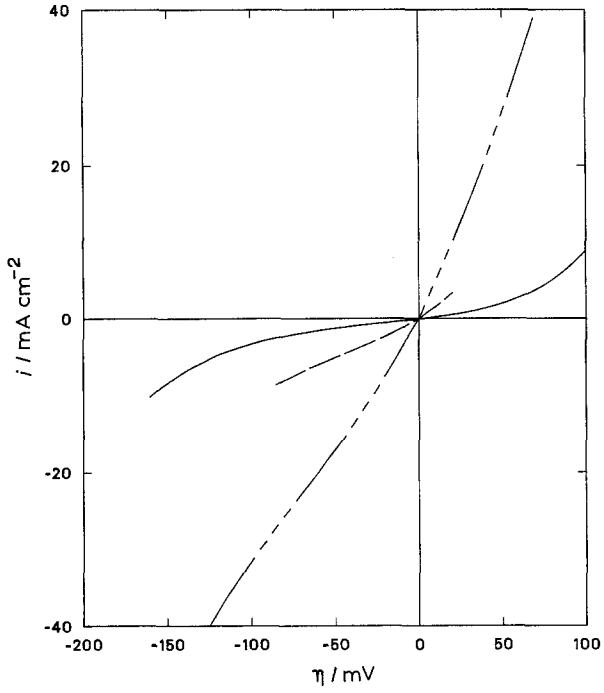

Fig. 9. Current density against overpotential on two cobalt-electroplated 100-mesh nickel screens, at 1 dm^3 min^{-1} flow rate. Temperature: (——) 23° C; (– – –) 46° C; and (— — — —) 65° C.

ponse changed with repeated scans at 46° C. The electrodes were held at open circuit for 10 min between each scan, and the current reached a steady-state value after the 6th scan. After the initial corrosion of the nickel electrodes at 46° C, no further change in response with time was noted. The nickel electrodes were examined when the cell was disassembled; the metallic luster of the original electrodes was replaced by a grey-black coating, which did not peel off the electrode. Examination with a powder X-ray diffractometer could not detect lines due to any NiS_x phase above the nickel background lines. This evidence suggests that a thin layer of sulphide was probably formed *in situ* during the experiment. The layer is catalytic toward the polysulphide redox reaction and probably is protective of the nickel surface (at least on the time scale of the experiments, here several hours).

Figure 9 presents results of experiments that used two nickel screens electroplated with cobalt. The electrolyte was 1.3 M S^{2-}, 1 M S^0 at pH 12. Unlike the nickel screens, the response at the cobalt plated screens did not change with time. Visual examination of these screens after the experiment showed some loss of metallic luster. This might be due to sulphidation of the underlying nickel due to incomplete coverage by the cobalt plate. The Co and MoS_2 responses were similar. Table 3 compares the current density at −50 mV overpotential on MoS_2 and Co. The design goal of 10 to 20 mA cm^{-2} at 50 mV overpotential can be met using these electrodes.

4. Summary and conclusions

Previous work has demonstrated that porous electrodes are required for the counter electrode in a PEC utilizing the aqueous sulphide/polysulphide redox couple in order to meet a design goal of supporting 10 to 20 mA cm^{-2} at less than 50 mV overpotential. A flow cell for testing flow-through porous electrodes was designed and constructed. The cell had an upstream counter electrode and a reference electrode, the electrolyte flow rate could be controlled precisely from 0.1 to 1.6 dm^3 min^{-1}, and the temperature of the system could be varied from room temperature to 80° C. Pt–10% Rh electrodes and a 10 mM $K_3Fe(CN)_6/K_4Fe(CN)_6$ in 1 M KCl electrolyte were used to test the mass-transfer characteristics of the system. The measured mass-transfer coefficients were generally in accord with previous work, however the value of the Sherwood number obtained was slightly higher.

Nickel wire-mesh electrodes and molybdenum expanded-metal mesh electrodes were used in the aqueous polysulphide electrolyte. The molybdenum had a MoS_2 layer grown by reaction with sulphur vapour at 450° C, and some of the nickel screens were plated with cobalt. The effect of electrode material, temperature, flow rate, and the addition of DMF were studied. Flow rate variation between 0.1 and 1.6 dm^3 min^{-1} had only a small effect on the current density–overpotential curves. Raising the temperature and/or the addition of DMF had much larger effects. These observations are in accord with the prior steady-state results obtained on rotating disc electrodes. The nickel electrodes showed some evidence of inital corrosion. The cobalt and MoS_2 electrodes gave similar responses which were more than adequate to meet the design goals.

Acknowledgement

This work was supported by the Assistant Secretary for Conservation and Renewable Energy, Deputy Assistant Secretary for Utility Technologies, Office of

Table 3. Performance of Co and MoS_2 electrodes: current density (mA cm^{-2}) at −50 mV overpotential

Temperature /° C	*Two 100-mesh Ni screens plated with Co (no DMF)*	*Two Mo expanded metal mesh screens with a deposited MoS_2 layer (no DMF)*	*Two Mo expanded metal mesh screens with a deposited MoS_2 layer (13 mol % DMF)*
25	−1.2	−0.8	−2.4
46	−5.0	−3.2	−14.6
65	−17	−9.2	−28.6
79	-	−20.5	−39.0

Energy Management, Advanced Utility Concepts Division of the U.S. Department of Energy under Contract No. DE-AC03-76SF00098.

References

[1] G. Schwarzenbach and A. Fischer, *Helv. Chim. Acta.* **43** (1960) 1365.
[2] A. Teder, *Acta Chem. Scand.* **25** (1971) 1722.
[3] W. Giggenbach, *Inorg. Chem.* **11** (1972) 1201.
[4] A. Teder, *Ark. Kemi* **30** (1969) 379.
[5] *Idem, ibid.* **31** (1969) 173.
[6] S. Licht, G. Hodes, and J. Manassen, *Inorg. Chem.* **25** (1986) 2486.
[7] A. Teder, Sv. *Papperstidn.* **71** (1968) 149.
[8] Z. V. Bogomolova, K. I. Tikhonov, and A. L. Rotinyan, *Elekrokhimiya* **15** (1979) 1237.
[9] P. Lessner, J. Winnick, F. R. McLarnon and E. J. Cairns, *J. Electrochem. Soc.* **133** (1986) 2510.
[10] *Idem, ibid.* **133** (1986) 2517.
[11] *Idem, ibid.* **134** (1987) 2669.
[12] N. Ardoin and J. Winnick, *ibid.* **135** (1988) 1719; J. Winnick, P. M. Lessner, F. R. McLarnon and E. J. Cairns, *Appl. Phys. Lett.* **53** (1988) 1985.
[13] M. Matlosz and J. Newman, 'Use of a Flow-Through Porous Electrode for Removal of Mercury from Contaminated Brine Solutions,' *in* 'Transport processes in electrochemical systems,' (edited by R. S. Yeo, T. Katan and D. T. Chin), The Electrochemical Society Symposium Proceeding Series, The Electrochemical Society, Pennington, NJ (1982) p. 53.
[14] M. A. Reid and L. H. Thaller, 'Improvement and Scale-Up of the NASA Redox Storage System,' Proceedings of the 15th Intersociety Energy Conversion Engineering Conference, American Institute of Aeronautics and Astronautics, New York (1980) p. 1471.
[15] M. Barak, 'Electrochemical Power Sources. Primary and Secondary Batteries,' Institution of Electrical Engineers, London (1980).
[16] G. Hodes, J. Manassen, and D. Cahen, *J. Electrochem. Soc.* **127** (1980) 544.
[17] *Idem, J. Appl. Electrochem.* **7** (1977) 181.
[18] R. J. Remick and E. H. Camara, 'Electrochemistry of the Sulfide/Polysulfide Couple,' Lawrence Berkeley Laboratory Report No. LBL-16850 (1983).
[19] P. L. Allen and A. Hickling, *Trans. Faraday Soc.* **53** (1957) 1626.
[20] J. C. Armour and J. N. Cannon, *AIChE J.* **14** (1968) 415.
[21] Anonymous, *Electroplating* **3** (1951) 89.
[22] J. E. Dutrizac, *Can. Met. Quart.* **9** (1970) 449.
[23] R. E. Sioda, *Electrochim. Acta.* **22** (1977) 439.
[24] J. Cano and U. Böhm, *Chem. Eng. Sci.* **32** (1977) 213.